Jurnal Teknologi

Full Paper

RESPONSE OF FBG-BONDED GRAPHENE PLATE AT DIFFERENT APPLIED STRESS LOCATION

Younis Mohammed Salih*, Yusof Munajat, Abd. Khamim Ismail, Hazri Bakhtiar

Faculty of Science, Universiti Teknologi Malaysia, 81310 UTM Johor Bahru, Johor, Malaysia

Article history
Received
15 August 2015
Received in revised form
15 November 2015
Accepted
30 December 2015

*Corresponding author
Younis20000@gmail.com

Graphical abstract

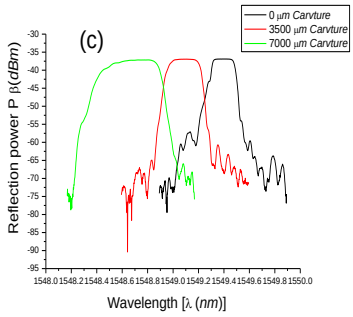

Abstract

In this study, the response of a FBG-bonded-graphene plate at different applied stress location is demonstrated. The sensing element utilized for this purpose is a 35.9-*mm* FBG sensor bonded onto the surface of a graphene plate. The lateral displacement is changed with corresponding increase or decrease in the FBG's curvature. The change in center wavelength of the reflected spectrum is almost linear, without a significant hysteresis effect. It was also observed that the sensitivity of the FBG changes for location of applied stress. Likewise, the area under the reflection curve is observed to increase with increase in strain level, indicating an increase total power reflected. This is verified by an increase in the voltage output as observed from the oscilloscope.

Keywords: FBG, graphene, shift in Bragg wavelength

Abstrak

Dalam kajian ini, kesan apabila tekanan dikenakan pada lokasi yang berbeza di antara gentian belauan Bragg (FBG) yang dilekatkan bersama plat graphene dilakukan. Untuk tujuan ini, elemen pengesan yang digunakan ialah pengesan FBG 35.9 *mm* dilekatkan pada permukaan plat graphene. Sisi anjakan spektrum didapati berubah dengan kadar kelenturan FBG. Perubahan pada panjang gelombang pusat sesuatu spektrum yang terpantul adalah hampir selari pada tiap kelenturan tanpa ada kesan histerisis yang besar. Kajian juga mendapati sensitiviti FBG berubah pada setiap lokasi tekanan yang dikenakan. Begitu juga dengan kawasan di bawah spektrum yang terpantul, ia bertambah besar apabila tahap tekanan meningkat dimana terdapat peningkatan pada jumlah kuasa yang terpantul. Hal ini dapat dibuktikan dengan berlakunya peningkatan pada keluaran voltan seperti yang dapat dilihat daripada osiloskop.

Kata kunci: FBG, graphene, anjakan di dalam Bragg panjang gelombang

1.0 INTRODUCTION

In 1978, at the Canadian Communications Research Centre (CRC) in Ottawa, Ontario, Canada, [1] first demonstrated the formation of permanent grating structures in optical fiber . A Fiber Bragg Grating (FBG) is fabricated by constructing periodic or quasi periodic changes in the refractive index of the core along a single mode optical fibre length. This periodic change in refractive index is typically created by exposing the core to an intense optical interference pattern of ultraviolet energy. After which the pattern is printed into the fiber [2-4].

In recent years, because of the potential of FBGs as underwater acoustic sensors, many of researchers have developed experimental studies with the aim of finding sensors without explosion or inferior fire proof due to the piezoelectric effect. The factors that drive this research

effort are mainly because of the multiple advantages FBGs have over conventional sensors. Some of these characteristics include; high sensitivity, electrically passive operation, wide dynamic range, light weight, Remote Sensing, immunity to electromagnetic interference, approximate point sensing, Long-Term Stability, multiplexing capabilities and embed ability. But the most distinguishing feature of fiber gratings is the flexibility they offer for achieving desired spectral characteristics, and have all the advantages normally attributed to fiber sensors [5-9].

Furthermore, an FBG device can easily be replace the dependence on piezo ceramic (lead zirconate titanatePZT) hydrophones to convert an acoustic wave into an output voltage. This is because, the electronic parts of the hydrophones, is subjected to continuous harm and degradation when immersed in water. In addition, the wiring that is a characteristic of hydrophones makes the final device heavy and bulky. This can also be simplified by the use of FBG [10].

Montero *et al*., (2011), the feasibility of calculating strains in aged F114 steel specimens with Fiber Bragg Grating (FBG) sensors and infrared thermography (IT) techniques was studied [11]. Two specimens were conditioned under extreme temperature and relative humidity conditions making comparative tests of stress before and after aging, using different adhesives. Wu and Okabe, (2012), the demonstration of a high-sensitivity ultrasonic sensing system was proposed. In their system, a phase-shifted fiber Bragg grating (PS-FBG) was used as a sensor to achieve broadband and highly sensitive detection [12].

In this paper, we focus on the response of FBG - bonded graphene plate at different applied stress location.

With the thickness of a single layer of ~0.335 nm, as at now, graphene is the thinnest film in the universe. Graphene has very high mechanical strength and can be stretched by as much as 20%. Ma *et al*., (2012) have shown that with such a unique characteristics of graphene, it is possible to build miniature pressure and acoustic sensors with high sensitivity and dynamic range [13].

Suk *et al*., (2010) Have shown that a Monolayer graphene oxide has a lower effective Young's modulus (207.6±23.4 GPa when a thickness of 0.7 nm is used) as compared to the value reported for "pristine" graphene. The prestress (39.7-76.8 MPa) of the graphene oxide membranes obtained by solution-based deposition was also found to be 1 order of magnitude lower than that obtained by others for mechanically cleaved graphene. The presented unique AFM imaging and FEM-based mapping methods can be general utilized for obtaining the elastic modulus and prestress of thin membranes [14].

Fiber gratings can be broadly classified into two types: Bragg gratings (also called reflection and short-period gratings), in which coupling occurs between modes traveling in opposite directions; and transmission gratings (also called long-period gratings), in which the coupling is between modes traveling in the same direction [7].

These types of uniform fibre gratings, where the phase fronts are perpendicular to the fibres longitudinal axis with grating planes. The Bragg grating condition is simply the requirement that satisfies both energy and momentum conservation. The first-order Bragg condition is defined as [15].

$$\lambda_\beta = 2\, n_{eff}\ \Lambda \tag{1}$$

Where

λ_β = Bragg wavelength; Λ = Grating period; n_{eff} = Effective refractive index of the grating in the fiber core.

From Eq. (1) a change in the Bragg wavelength λ_β can be achieved by either a change in the grating period, Λ, or a change in the effective refractive index, n_{eff} That is,

$$\Delta\lambda_\beta = 2n\Delta\Lambda + 2\Lambda\Delta\, n_{eff} \tag{2}$$

For the specific case of pure axial loading, the shift in Bragg wavelength is linearly related to the applied axial strain that can be written as,

$$\Delta\lambda_\beta = \lambda_\beta\ (1 - P_e)\epsilon \tag{3}$$

Where P_e is the effective photo-elastic constant for axial strain with a typical value 0.22

We can thus represent Eq. (3) by the following expression:

$$\Delta\lambda_\beta\ /\ \lambda_\beta = 0.78\epsilon \tag{4}$$

From Eq. (4) FBGs are typically utilized as spectral transduction elements, where the change in the measure is detected via a shift in the peak wavelength of the FBG (in the case of hydrophones) or in the form of a strain wave (for mechanical vibrations), to be converted into the shift in the wavelength which can easily be determined via an interrogator [16, 17].

1.2 Interrogation Methods

For the acoustic wave detection, a new and fast interrogation system is needed. The working principle of fiber optic sensor using FBG (Fiber Bragg Grating) was shown in Figure 1, [27]. Also, for more illustration, a transmission spectrum is shown on the left in the Figure 2. From the graph, it can easily be observed that, as the Bragg wavelength increases from λ_1 to λ_2, the transmitted intensity decreases while the reflected or rejected intensity increases accordingly.

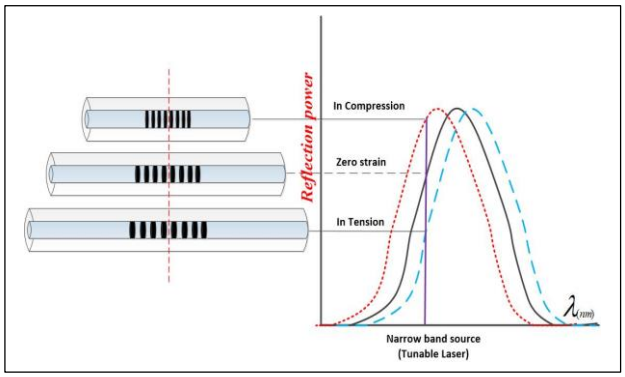

Figure 1 Measuring principle of FBG sensor

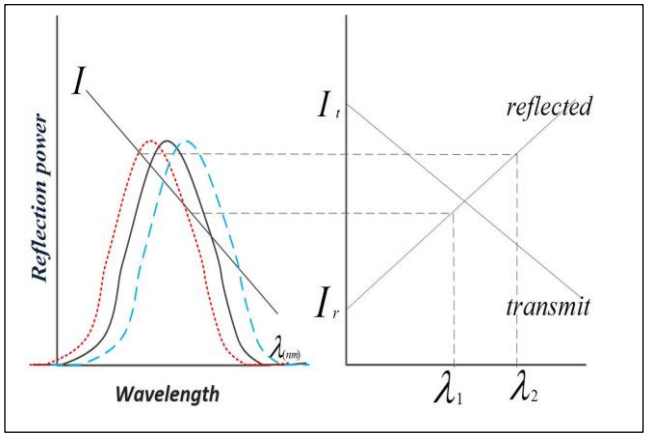

Figure 2 Demodulating FBG with a passive filter. Wavelength shifts (left) are converted into intensity changes (right) [18]

Lee and Jeong, (2002), many interrogation techniques for fiber grating sensors and the theory of fiber gratings were mentioned [19]. Essentially, two broad interrogation methods are available for the detection of high frequency acoustic signal with FBGs which are, power detection methods, and edge filter detection methods [16].

1.2.1 Power Detection Methods

With respect to power detection methods as used in this work, the shift in the FBG peak wavelength (the Bragg wavelength) is detected due to the spectral properties of the Light Source (LS). When power detection method is used, the FBG acts as a filter that splits the incident optical power into a reflect component and a transmit component. As the applied measure changes the Bragg wavelength, the total power transmitted and reflected is also changed [17]. Power detection methods are two, the linear edge source [19] and the narrow bandwidth source [20].

As illustrated in Figure 3a, in the case of linear edge source power detection, the edge of a relatively broadband source (source bandwidth > FBG bandwidth), and the FBG is chosen such that the Bragg wavelength is located at the 3dB point of the source. The wavelength shift of the FBG will then produce a direct change in the reflected intensity as it shifts up and down the edge of the source's spectrum [16].

The second power detection method is the opposite of the linear edge source (Figure 3b). In this case, a relatively narrow bandwidth source (source bandwidth < FBG bandwidth) is set to the 3dB point of the FBG. In this case, either the reflect power can be utilized [20], or the transmitted power can be utilized [21].

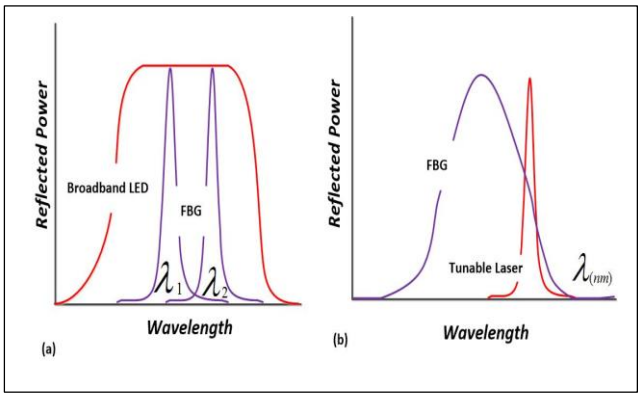

Figure 3 FBG detection method using: (a) a broadband light emitting diode; (b) a narrow line-width tunable laser source [17]

1.2.2 Edge Filter Detection Methods

For edge detection methods, a spectrally-dependent filter which results in a change in intensity at the detector is used to detect the shift in the FBG spectrum. Illumination of the FBG is done by a broadband source like SLD. The change in the reflected wavelength causes variation in the transmitted intensity since the filter's transmittance varies as a function of wavelength. In this case, the kinds of filters that can be utilized include; a matched FBG [23], a Wavelength division multiplexing (WDM) coupler [24], an Arrayed-waveguide (AWG) [25] and a dense division multiplexing (DWDM) filter [26]. numbers.

The most straight-forward of the edge filter detection methods is the linear edge absorption filter. This is mainly because an external filter is used. While the simplest form of the edge filter is a matched FBG. In this case, an identical FBG is used as the filter which converts the spectral shift of the FBG into an intensity change. Other two edge filter detection methods are AWG and DWDM filter which are both multichannel devices can be classified as identical in their implementation [16].

2.0 METHODOLOGY

2.1 Preparation of FBG-bonded Sensor

A 35.9-*mm* FBG sensor is bonded onto the surface of a graphene plate. Then, SELLEEYS type of adhesive is used to locate graphene plate from ends on the plastic rulers with the FBG horizontally bonded on graphene plate, as illustrated in Figure 4.

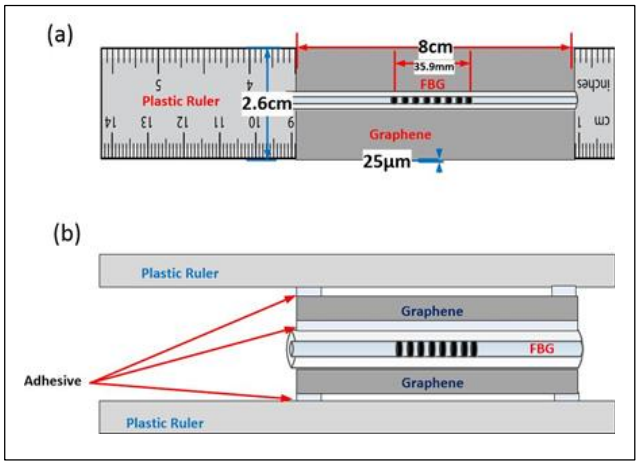

Figure 4 FBG bonded on graphene plate. (a) Ruler, graphene and FBG dimensions. (b) Explanation FBG bonded on graphene and graphene with rulers

2.1 Compression and Curvature Effect on FBG

In order to determine the effect of compression and curvature on a FBG (1549.39 *nm*), an external power source (ALS-18-B-FA ASE) with a spectral range of 1528 *nm* to 1564 *nm* and operating at maximum power, is used as a light source (LS). Port 1 and port 2 of a circulator are connected to the LS and the FBG sensor respectively. Then, by changing the displacement in linear translation stage (in amount of μm), the reflection spectrum of the disturbed FBG will be obtained in two ways; i) by using an optical spectrum analyzer (OSA), ii) second by using a high-speed photo diode together with an oscilloscope.

In the first stage of the experiment, in steps of 250μm the lateral displacement is changed from (0μm to 7000μm), with corresponding increase or decrease in the FBG's curvature. The change in center wavelength (Bragg wavelength shift caused by compression and curvature) of the FBGs is recorded in , for the stress-location at 1cm away from the end of the FBG region. In addition, the experiment is repeated for stress-locations at 2cm and 3cm. The reflected spectrum is taken for three different lateral displacements (0μm, 3500μm and 7000μm). Figure 5 illustrates the experimental setup for determining the response of compression and curvature on the FBG. A (Yokogawa AQ6370C) optical spectrum analyzer (OSA) is utilized in this experiment.

In the second stage of the experiment, a high-speed photo diode together with an oscilloscope is used instead of the OSA. For a similar in lateral displacement as above, and a corresponding increase and decrease in the curvature of the FBG, the change in mean voltage is observed and recorded. Figure 5 the discontinuous line represents the setup for obtaining the curvature compression of the FBG. The specification for the High-Speed photo diode used is (DET01CFC), having wavelength of (800 – 1700 *nm*) and the oscilloscope used was REGOL DS2000.

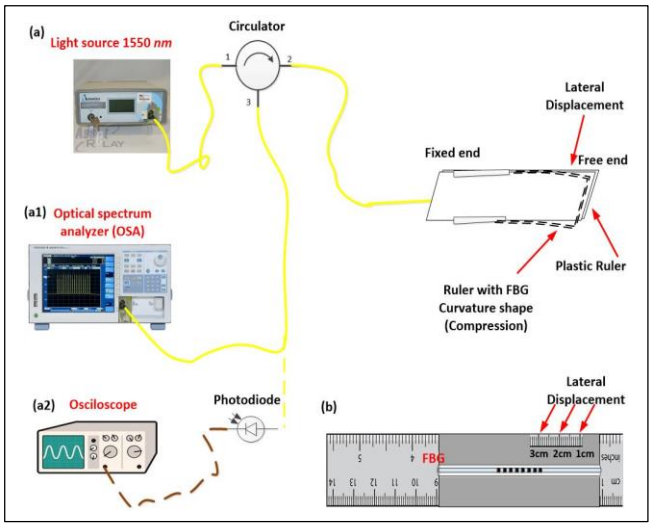

Figure 5 (a) Experiment set up of compression and curvature effect on FBG. (a1) using (OSA) to retrieve the reflected spectrum data. (a2) using oscilloscope to record the change in the voltage, the discontinuous line represents using oscilloscope to record the change in the voltage. (b) Location of applied stress

3.0 RESULTS AND DISCUSSION

3.1 Center Wavelength Shift for Various Compression and Curvature of 35.9 *mm* FBG

A graph of center wavelength against lateral displacement is plotted as given in Figure 6, for the three stress-locations. A decrease in centre wavelength is observed when the displacement is increased. The slope changes with the location of the applied stress, the slope value at (1cm, 2cm and 3m) are (-6.85x10^{-5} $nm/\mu m$, -7.66x10^{-5} $nm/\mu m$ and -8.44x10^{-5} $nm/\mu m$) respectively, indicating the sensitivity of the FBG increases as the stress-location become closer to the FBG. No hysteresis effect is observed at each stress-location, since there is no significant change in the slope, when the displacement is increased or decreased.

3.2 Output Power of Reflected Signal for Various Compression and Curvature

Figure 7 shows the reflection spectrum from the OSA for each applied stress location. It shows an increase in width and area under the reflected curve, indicating that the power increases as the curvature increases. As the displacement increases, more power is being reflected.

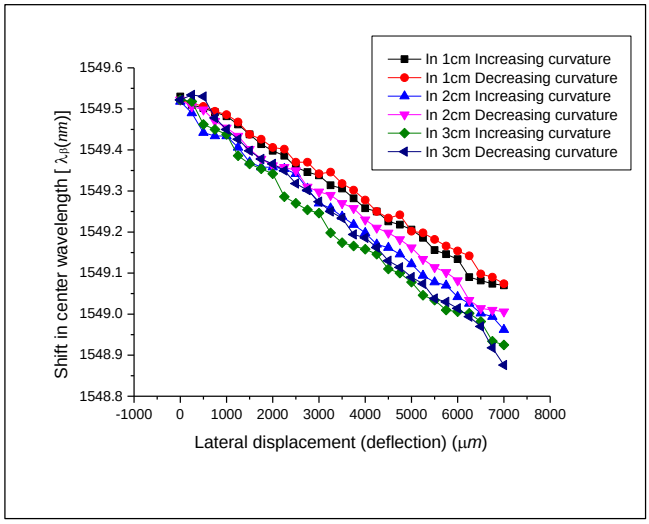

Figure 6 Centre wavelength shift λ_β for various compression and curvature of FBG, at different applied stress location, (1cm, 2cm, and 3cm) far away from the end of FBG region

Calculation results using the Origin program 9 shows an increase in area under the reflection curve, as shown in Table 1. If that total area represents the total output reflected power coming from the FBG, then it is expected that the output reflected power received by the photodiode should also increase correspondingly.

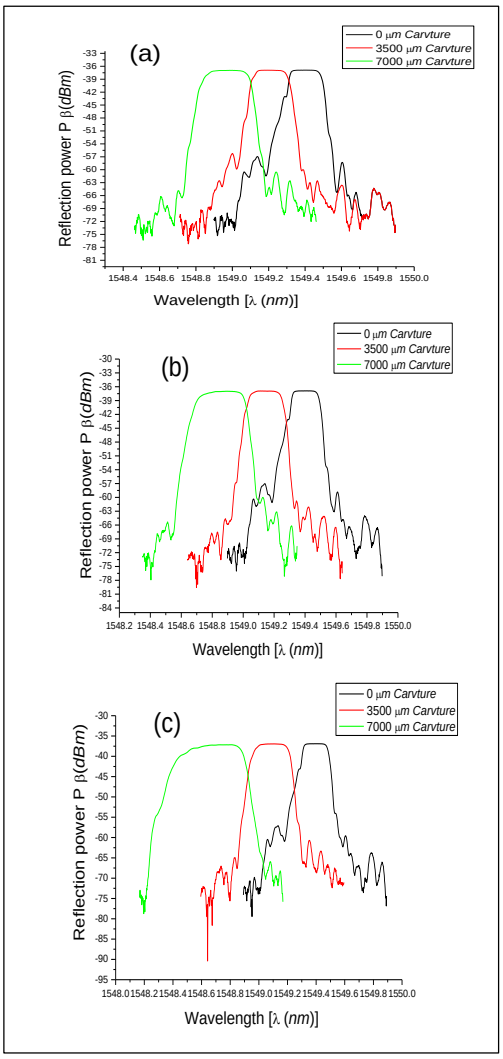

Figure 7 Reflected spectrum power for various compression and curvature of 35.9*mm* FBG, at different applied stress location, [a) at 1cm, b) at 2cm, and c) at 3cm] far away from the end of FBG region

Table 1 Variation of area with locations

Displacement	1cm Location	2cm Location	3cm Location
0 μm	15.5784	16.76233	18.25809
3500 μm	15.7899	18.41586	23.26135
7000 μm	17.42957	22.30816	28.42512

3.3 Reflected Voltage for Various Compression and Curvature of 35.9 *mm*

Figure 8 shows the graph of average voltage from Oscilloscope against lateral displacement. The expected increase in output reflected power is clearly visible from the graph. So both the calculation result (Table 1) and the experimental measurement support each other.

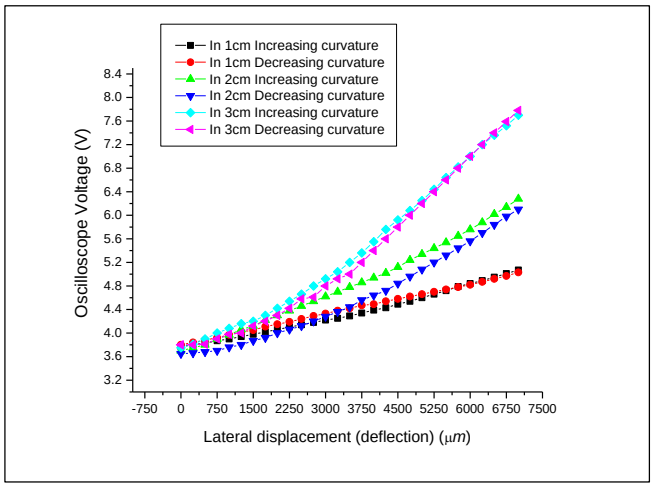

Figure 8 Output voltage for various compression and curvature of 35.9*mm* FBG, at different applied stress location, 1cm, 2cm, and 3cm) far away from the end of FBG region

4.0 CONCLUSION

In this work, the response of FBG-bonded graphene plate at different applied stress location was investigated. The lateral displacement applied on the graphene-plate with the bonded FBG, Causes the curvature of the plate to increase or decrease. Two experimental procedure were performed to obtain either the wavelength shift from the reflected spectrum of the FBG (using an OSA) or the Voltage output for the same FBG (using an oscilloscope). The findings concluded from the investigation can be summarized in three points:

(a) The sensitivity of the FBG changes with the location applied stress. As the location approaches the location of the FBG, the sensitivity of FBG (magnitude of change) increases from 1.85x10^{-4}*V.μm*$^{-1}$, to 5.83x10^{-4} *V.μm*$^{-1}$.

(b) From the reflection spectrum the output power increases as the location of applied stress approaches to location of the FBG, as shown by the increase in the area of the reflection spectrum.

(c) The result correspond to the increase in output voltage power as detected by the photodiode. There is a clear correlation between the optical and electrical outputs observed.

Acknowledgement

The authors would like to thank the Malaysian Ministry of Higher Education and Universiti Teknologi Malaysia for their financial funding through GUP vote number Q.J130000.2509.08H40.This support is gratefully acknowledged.

References

[1] Hill, K., Fujii, Y., Johnson, D. C. and Kawasaki, B.1978. Photosensitivity In Optical Fiber Waveguides: Application To Reflection Filter Fabrication. *Applied Physics Letters*. 32(10): 647–649.

[2] Hill, K. O. and Meltz, G. 1997. Fiber Bragg Grating Technology Fundamentals And Overview. *Lightwave Technology, Journal of*. 15(8): 1263-1276.

[3] Skaar, J. 1978. Synthesis And Characterization Of Fiber Bragg Gratings. *NTNU. 2000*. 32(10): 647-649.

[4] Mastro, S. A. 2005. Optomechanical Behavior Of Embedded Fiber Bragg Grating Strain Sensors. Ph.D. Thesis. Drexel University.

[5] Takahashi, N., Tetsumura, K. and Takahashi, S. 1999. Underwater Acoustic Sensor Using Optical Fiber Bragg Grating As Detecting Element. *Japanese Journal Of Applied Physics*. 38: 3233.

[6] Kersey, A. D., Davis, M. A., Patrick, H. J., LeBlanc, M., Koo, K., Askins, C., Putnam, M. and Friebele, E. J. 1997. Fiber grating sensors. *Lightwave Technology, Journal of*. 15(8): 1442-1463.

[7] Erdogan, T. 1997. Fiber Grating Spectra. *Lightwave Technology, Journal of*. 15(8): 1277-1294.

[8] Li, H.-N., Li, D.-S. And Song, G.-B. 2004. Recent Applications Of Fiber Optic Sensors To Health Monitoring In Civil Engineering. *Engineering Structures*. 26(11): 1647-1657.

[9] Oswald, D., Richardson, S. and Wild, G. 2011. Numerical Modelling Of Interrogation Systems For Optical Fibre Bragg Grating Sensors. *Smart Nano-Micro Materials and Devices. International Society for Optics and Photonics*. 82040Q-82040Q.

[10] Moccia, M., Pisco, M., Cutolo, A., Galdi, V., Bevilacqua, P. and Cusano, A. 2011. Opto-Acoustic Behavior Of Coated Fiber Bragg Gratings. *Optics Express.* 19(20): 18842-18860.

[11] Montero, A., Saez de Ocariz, I., Lopez, I., Venegas, P., Gomez, J. and Zubia, J. 2011. Fiber Bragg Gratings, IT Techniques and Strain Gauge Validation for Strain Calculation on Aged Metal Specimens. *Sensors*. 11(1): 1088-1104.

[12] Wu, Q. and Okabe, Y. 2012. High-Sensitivity Ultrasonic Phase-Shifted Fiber Bragg Grating Balanced Sensing System. *Optics Express.* 20(27): 28353-28362.

[13] Ma, J., Jin, W., Ho, H. L. and Dai, J. Y. 2012. High-Sensitivity Fiber-Tip Pressure Sensor With Graphene Diaphragm. *Optics Letters*. 37(13): 2493-2495.

[14] Suk, J. W., Piner, R. D., An, J. and Ruoff, R. S. 2010. Mechanical Properties Of Monolayer Graphene Oxide. *ACS Nano*. 4(11): 6557-6564.

[15] Othonos, A. 1997. Fiber Bragg Gratings. *Review Of Scientific Instruments*. 68(12): 4309-4341.

[16] Wild, G. and Hinckley, S. 2010. Optical Fibre Bragg Gratings For Acoustic Sensors. *International Congress On Acoustics (ICA)*. 23-27.

[17] Wild, G. and Richardson, S. 2012. Optimisation of Power Detection Interrogation Methods for Fibre Bragg Grating *Sensors*.

[18] http://www.smartfibres.com/interrogationtechniques

[19] Lee, B. and Jeong, Y. 2002. Interrogation Techniques For Fiber Grating Sensors And The Theory Of Fiber Gratings. *Fiber Optic Sensors.* 2002: 295-381.

[20] Webb, D. J., Surowiec, J., Sweeney, M., Jackson, D. A., Gavrilov, L., Hand, J., Zhang, L. and Bennion, I. 1996. Miniature Fiber Optic Ultrasonic Probe. *SPIE's 1996 International Symposium on Optical Science, Engineering, and Instrumentation. International Society for Optics and Photonics.* 76-80.

[21] Takahashi, N., Hirose, A. and Takahashi, S. 1997. Underwater Acoustic Sensor With Fiber Bragg Grating. *Optical Review.* 4(6): 691-694.

[22] Lin, B. and Giurgiutiu, V. 2014. Development Of Optical Equipment For Ultrasonic Guided Wave Structural Health Monitoring. SPIE Smart Structures and Materials+ Nondestructive Evaluation and Health Monitoring. *International Society for Optics and Photonics.* 90620R-90620R.

[23] Perez, I. M., Cui, H. and Udd, E. 2001. Acoustic Emission Detection Using Fiber Bragg Gratings. SPIE's 8th Annual International Symposium on Smart Structures and Materials. *International Society for Optics and Photonics*. 209-215.
[24] Ambrosino, C., Diodati, G., Laudati, A., Gianvito, A., Sorrentino, R., Breglio, G., Cutolo, A., Cusano, A. 2007. Active Vibration Control Using Fiber Bragg Grating Sensors And Piezoelectric Actuators In Co-Located Configuration. Third European Workshop on Optical Fibre Sensors. *International Society for Optics and Photonics*. 661940-661940.
[25] Fujisue, T., Nakamura, K. and Ueha, S. 2006. Demodulation Of Acoustic Signals In Fiber Bragg Grating Ultrasonic Sensors Using Arrayed Waveguide Gratings. *Japanese Journal Of Applied Physics*. 45(5S): 4577.
[26] Lin, B. and Giurgiutiu, V. 2013. Exploration of Ultrasonic Guided Wave Detection with Optical Fiber Sensors and Piezoelectric Transducers. *Proc. 9th International Workshop on Structural Health Monitoring, IWSHM*.1559-1566.
[27] Seo, D.-C., Yoon, D.-J., Kwon, I.-B.and Lee, S.-S. 2009. Sensitivity Enhancement Of Fiber Optic FBG Sensor For Acoustic Emission. *The 16th International Symposium on: Smart Structures and Materials & Nondestructive Evaluation and Health Monitoring. International Society for Optics and Photonics.* 729415-729415.